Canadian Science Publishing

ARTICLE

Revisiting interpretation of relative density from shallow depth CPTs in sand

Lone Krogh, Santiago Quinteros, Harun Kursat Engin, and Tom Lunne

Can. Geotech. J. Downloaded from cdnsciencepub.com by NORWEGIAN GEOTECHNICAL INSTITUTE (NGI) on 05/02/23

Abstract: The relative density is an important state parameter in the determination of engineering properties of marine sands. Existing industry-acknowledged cone penetration test (CPT) correlations to relative density have been developed almost exclusively from the results of calibration chamber testing performed at stress levels higher than 50 kPa. A few studies suggest correlations for low stress levels as well, however, mainly for unaged normally consolidated soils. Existing formulations are often found to be challenged in the application for dense to very dense aged overconsolidated marine sands. This paper investigates the conditions and response of overconsolidated medium dense to very dense sand (as typically found in the North Sea) at shallow depths (less than 50 kPa) for a penetrating cone. It provides recommendations for a consistent set of parameters linking CPT parameters to the stress conditions, expressed by the apparent overconsolidation ratio and coefficient of earth pressure at rest, and the relative density. The recommendations are based on a comprehensive field-testing campaign at a sand site in Cuxhaven, Germany, supported by a suite of laboratory testing and numerical analyses.

Key words: relative density, cone penetration test (CPT), sand, overconsolidated, shallow depth, offshore, density.

Résumé : Il est essentiel de déterminer la densité relative comme paramètre d'état pour déterminer les propriétés techniques des sables marins. Le processus de corrélation entre l'essai de pénétration au cône (CPT) et la densité relative, reconnu par l'industrie, a été développé presque exclusivement à partir des résultats d'essais en chambre d'étalonnage réalisés à des niveaux de contrainte supérieurs à 50 kPa. Quelques études suggèrent des corrélations pour des niveaux de contrainte faibles aussi, cependant, principalement pour les sols non vieillis normalement consolidés. Il est fréquemment constaté que les formulations existantes ne sont pas adaptées à l'application de sables marins surconsolidés denses à très denses et vieillis. La présente étude porte sur les conditions et la réponse d'un cône de pénétration dans un sable surconsolidé moyennement dense à très dense (comme on en trouve généralement en mer du Nord) à faible profondeur (moins de 50 kPa). L'étude fournit des recommandations pour un ensemble cohérent de paramètres reliant les paramètres CPT aux conditions de contrainte, exprimées par le rapport de surconsolidation apparent et le coefficient de pression des terres au repos, et la densité relative. Les recommandations sont basées sur une campagne complète d'essais sur le terrain sur un site de sable à Cuxhaven, en Allemagne, soutenue par une série d'essais en laboratoire et d'analyses numériques. [Traduit par la Rédaction]

Mots-clés : densité relative, essai de pénétration au cône (CPT), sable, surconsolidation, faible profondeur, offshore, densité.

1. Introduction

Offshore wind developments involve increasingly larger wind turbine generators at deeper waters along with novel and shallower foundation solutions. Hence, not only the ultimate limit state, but also the serviceability limit state is now governing turbine foundation designs. Higher risks are further experienced in relation to the design and burial of subsea power cables, where the export cable routes are becoming even longer as well. These recent offshore advancements entail an accelerated focus on the investigations and assessments of the conditions and geotechnical properties of the shallow and uppermost metres of soil.

The cone penetration test (CPT) is the primary in situ site investigation tool for offshore wind, oil and gas developments as well as for many onshore construction sites. The stress–strength and stiffness parameters of sandy soils for facility designs cannot be measured directly with the CPT, but the CPT has proven useful for determining the in situ relative density (D_r) of deep loose to dense sand deposits (i.e., for vertical effective stresses >50 kPa). Appropriate in situ estimates of strength and stiffness for design can then be derived in combination with laboratory testing targeting in situ stress conditions and information about sand intrinsic characteristics, e.g., gradation, grain morphology and mineralogy.

Existing industry-acknowledged CPT correlations (e.g., Baldi et al. 1986 and subsequent paper Jamiolkowski et al. 2003) for deriving relative density in sand have been developed almost exclusively from results of calibration chamber (CC) tests performed at stress levels higher than 50 kPa. Additional studies have investigated correlations for low stress levels (<50 kPa), e.g., Puech and Foray (2002), Emerson et al. (2008), and Senders (2010). The methods have proved useful in correlating CPT parameters to relative density and strength in unaged normally consolidated (NC) silica sands. However, application of these correlations to dense to very dense aged and overconsolidated (OC) quartz sands as typically met in the North Sea tend to overestimate relative density, especially at the low stress levels.

Received 20 April 2021. Accepted 31 July 2021.

L. Krogh. Ørsted, Nesa Allé 1, 2820 Gentofte, Denmark.
S. Quinteros, H.K. Engin, and T. Lunne. Norwegian Geotechnical Institute (NGI), Oslo, Norway.
Corresponding author: Santiago Quinteros (email: saq@ngi.no).

© 2021 Author L. Krogh and NGI. This work is licensed under a Creative Commons Attribution 4.0 International License, which permits unrestricted use, distribution, and reproduction in any medium, provided the original author(s) and source are credited.

Can. Geotech. J. Downloaded from cdnsciencepub.com by NORWEGIAN GEOTECHNICAL INSTITUTE (NGI) on 05/02/23

Fig. 1. Comparison of q_c profiles from field and calibration chamber (CC) testing in normally consolidated (NC) and overconsolidated (OC) sands, respectively.

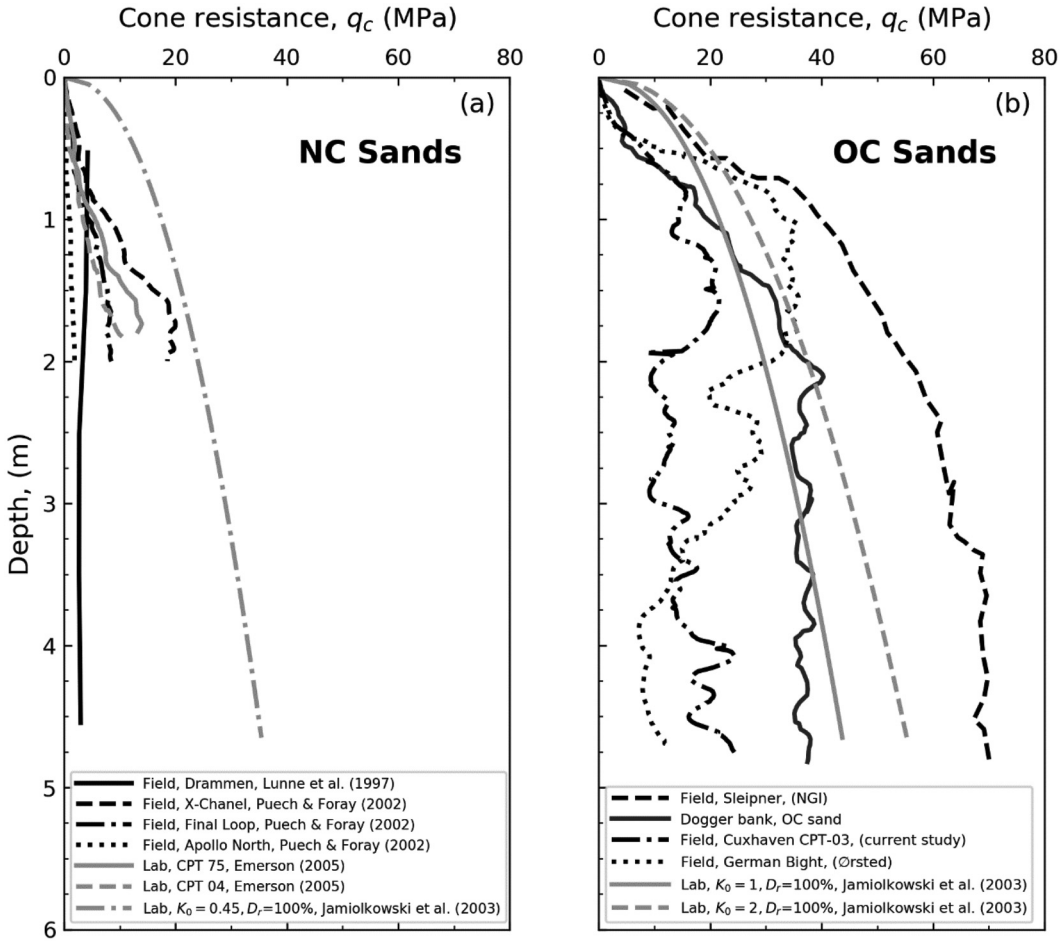

The fabric of sands achieved in a CC differs significantly from offshore field conditions, where a natural underwater deposition and compaction of the sands are further affected by years of impact of currents and wave loading as well as ageing. Figure 1 presents typical examples of measured cone resistances q_c as obtained in NC sands (both field and CC testing) compared to profiles in OC sands from various offshore in situ measurements. A q_c profile of an NC sand typically reaches a maximum of 15–20 MPa in the upper 2 m, whereas the q_c profile of an OC sand easily extends beyond 20–40 MPa with a distinct concave curvature at the uppermost 1–2 m depth.

This paper investigates the conditions of medium dense to very dense, either normally or overconsolidated, sand at low stress levels and the corresponding soil response during cone penetration. In the current study, seven cone penetration tests with pore pressure measurements (CPTUs) were conducted in a sand quarry with medium dense to very dense OC sand similar to a typical North Sea sand unit. The CPTUs were complemented by additional field testing and sampling for characterization of the sand and determination of stress history (Quinteros et al. 2018). Triaxial testing targeting in situ conditions were performed for determining the engineering properties and investigating various parameter dependencies (Quinteros et al. 2017). Numerical analyses with finite elements (FEs) (Engin et al. 2018) were performed for improving the understanding of the mechanical behaviour of a cone penetrating an OC sand and for extrapolating results of the physical testing beyond the physically tested conditions.

Fig. 2. Failure mechanisms associated with different phases of penetration (modified from Puech and Foray 2002).

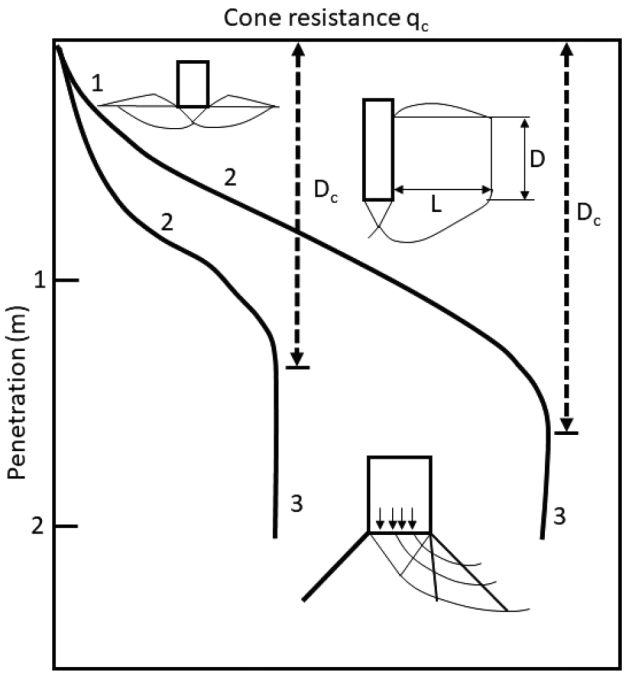

Can. Geotech. J. Downloaded from cdnsciencepub.com by NORWEGIAN GEOTECHNICAL INSTITUTE (NGI) on 05/02/23

Fig. 3. Sketch presenting field testing at surface level (depth 0.0 m) as distributed across testing area. [Colour online.]

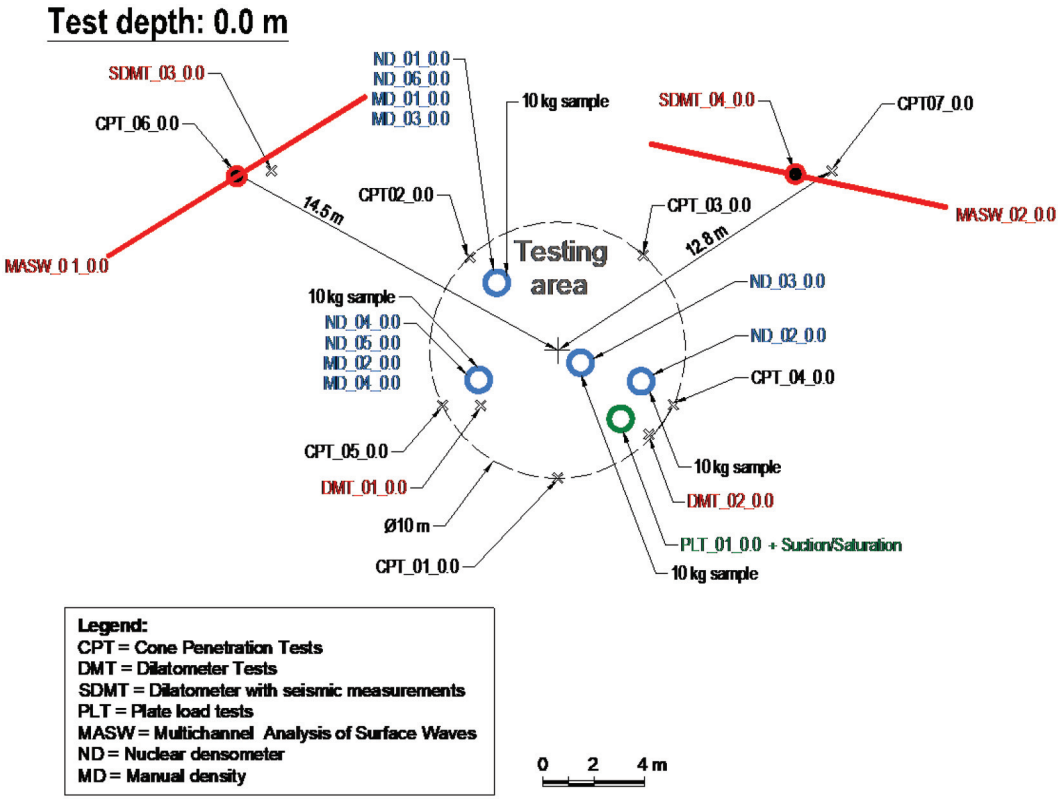

The paper provides a consistent set of parameters linking the measured CPT parameters to the in situ stress conditions, expressed by the apparent overconsolidation ratio (OCR) and the coefficient of earth pressure at rest (K_0), and D_r. The correlations are tried on typical examples of offshore CPT measurements and demonstrate that a rigorous assessment of the mean effective stresses is needed when interpreting shallow CPT data.

2. Background

A frequently applied CPT correlation to relative density has been proposed by Jamiolkowski et al. (2003) based on a comprehensive database of CC tests on Ticino, Toyoura, and Hokksund sands. Jamiolkowski et al. (2003) extended and improved the previous work done by Baldi et al. (1986) and proposed the following expression:

$$(1) \qquad q_c = C_0\left(\frac{\sigma'_m}{p_a}\right)^{C_1} e^{C_2 D_r} \quad \text{or} \quad D_r = \frac{1}{C_2}\ln\left[\frac{q_c}{C_0(\sigma'_m/p_a)^{C_1}}\right]$$

where C_0, C_1, C_2 are average fitting parameters for Ticino, Toyoura, and Hokksund sands, respectively, i.e., C_0 = 24.94, C_1 = 0.46, C_2 = 2.96, σ'_m is the mean effective stress = $(\sigma'_{vo} + 2\sigma'_{ho})/3 = (\sigma'_{vo}/3)(1 + 2K_0)$, and p_a is the atmospheric pressure (100 kPa). σ'_{vo} and σ'_{ho} are the in situ vertical and horizontal effective stresses, respectively. A constant value of K_0 = 1 is typically used in practice for OC sands with consideration to stress levels above 50 kPa.

Equation 1 is in principle limited to unaged, uncemented, air pluviated, fine to medium dry clean silica sand of low to moderate compressibility and primarily NC at vertical effective stresses above 50 kPa. Jamiolkowski et al. (2003) recommends the following relation between the dry and saturated relative densities, $D_{r,dry}$ and $D_{r,sat}$, respectively:

$$(2) \qquad \frac{D_{r,sat} - D_{r,dry}}{D_{r,dry}}100 = -1.87 + 2.32\ln\frac{q_c}{(\sigma'_v p_a)^{0.5}}$$

Equation 2 becomes meaningless when $q_c/(\sigma'_v p_a)^{0.5} \le 2.24$. The expression by Jamiolkowski et al. (2003) compares well with the correlation by Baldi et al. (1986) after correction for saturation effects, with differences of less than 10%.

With reference to the same CC data, Mayne (2009) presents an alternative formulation, which also considers overconsolidation and compressibility:

$$(3) \qquad D_r = 100\left[0.268\ln(q_{t1}) - b_x\right]$$

where q_{t1} is the normalized cone resistance $q_{t1} = q_t/(p_a\sigma'_v)^{0.5}$ and b_x = 0.675 from regression analyses on NC clean sands. For sands of high and low compressibility, respectively, b_x values of 0.525 and 0.825 are suggested, and overconsolidation can be accounted for by using $b_x = 0.675\text{OCR}^{0.2}$.

Puech and Foray (2002) presented a comprehensive attempt of assessing CPTs shallower than 3 m depth in terms of a nominal relative density and friction angle of marine sands. Puech and Foray (2002) investigated CPTs from CC tests on three silica sands (Hostun, Loire, and Fontainebleau), laboratory tests and back analysis of in situ offshore CPTs. Puech and Foray (2002) adopted the concept of a "critical depth", where q_c reaches a quasi-stationary value, as introduced by Biarez and Grésillon (1972). The method captures shallow CPT responses in NC silica sands, but appears to be inaccurate for denser OC sands. The method involves manual iterations, the use of empirical correlations, and is impractical for design works for multi-facility sites.

Emerson et al. (2008) expanded the work of Puech and Foray (2002) and suggested a "global approach" for estimating relative density at shallow and greater depths. The approach was validated using CC and laboratory testing, field data, and FE modelling.

Can. Geotech. J. Downloaded from cdnsciencepub.com by NORWEGIAN GEOTECHNICAL INSTITUTE (NGI) on 05/02/23

Fig. 4. CPTU results (modified from Quinteros et al. 2018).

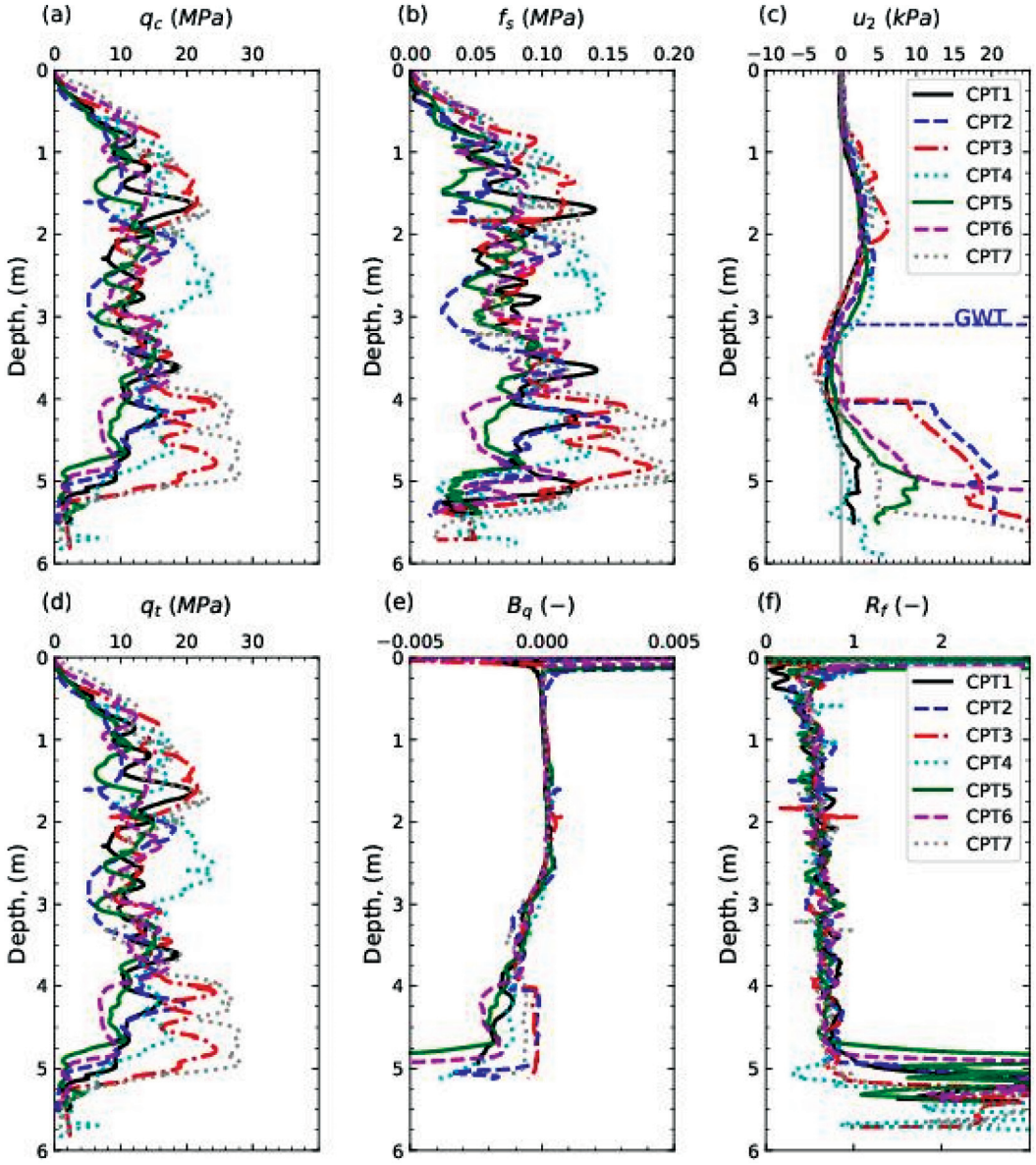

Emerson et al. (2008) proposed a three-phase interpretation (see Fig. 2); an initial phase (denoted 1 in Fig. 2) where shallow CPT conditions (dilative conditions) prevail, followed by a transitional phase (denoted 2 in Fig. 2) reflecting the change from a dilational to a compressional response at a critical stress level. Finally, a third phase (denoted 3 in Fig. 2) identifies the conditions at greater depths; the quasi-stationary phase. The approach by Emerson et al. (2008) involves the same advantages and limitations as Puech and Foray (2002).

Based on centrifuge testing Senders (2010) presents an approach for scaling or converting a q_c profile as measured with a laboratory mini-cone in an NC clean silica sand into a q_c profile as would be measured with a cone of different diameter in the same clean silica sand. Senders' approach combined correlations by Jamiolkowski et al. (1988) with a factor accounting for the influence of depth as well as cone diameter. The approach appears to capture typically observed sand behaviour at shallow depths.

The current study presents the results of a three-legged study consisting of field testing, laboratory testing, and FE analyses. The study was conducted for investigating the impact of overconsolidation on the CPT derived relative density of medium dense to very dense sands at shallow depths for obtaining an understanding of the uncertainties related to the use of existing methods with offshore conditions in mind.

3. Cuxhaven site characterization

3.1. Field testing

3.1.1. Site and field campaign

Shallow CPTUs and supplementary in situ testing were performed at a test field located approximately 5 km south of Cuxhaven, Germany, and 6 km east of the North Sea coast. The test site is part of a sand quarry consisting of a thicker layer of homogeneous OC sand. The pit started operations in 1980 and the total

Can. Geotech. J. Downloaded from cdnsciencepub.com by NORWEGIAN GEOTECHNICAL INSTITUTE (NGI) on 05/02/23

height of the excavated soil is roughly 18 m. Details of the site and the field works are presented in Quinteros et al. (2018).

The field testing comprised

- Seven CPTUs from 0 to 5 m depth.
- 34 nuclear densometer (ND) testing and 40 manual density (MD) push-in cylinder determinations using two different purpose-built sample cylinders at the surface of every 0.5 m excavation level.
- Soil sampling along every surface of each excavation level with measurements and monitoring of suction (using an MP-6 calibrated ceramic disk), volumetric water contents, and temperature (using a Decagon 5TM soil moisture–temperature probe).

The latter tests listed were performed at 0.5 m intervals to a depth of 3.67 m by a careful incremental excavation of the site. Figure 3 sketches the positions of the various tests relative to each other at surface level (test depth 0.0 m) and identifies further flat dilatometer testing (DMT), seismic dilatometer testing (SDMT), multichannel analysis of surface waves (MASW), and plate loading tests (PLTs). Results of DMT/SDMTs, PLTs, and MASW were valuable for the characterization of the site, but irrelevant for the analyses related to the CPT correlations to relative density (mainly due to their resolution with depth) and will thus not be referenced further.

The CPTUs were performed using a standard A.P. van den Berg 10 cm^2 cone measuring cone resistance (q_c), sleeve friction (f_s), and pore water pressure (u_2) at the cone shoulder. The tests were performed continuously with a standard penetration rate of 20 mm/s from ground level to termination depth (5 m).

Direct and indirect in situ density and water content measurements were performed using an ND (Troxler 3440) and by carefully sampling with small purpose-made sharp edged push-in cylinders (diameter Ø = 70 mm with lengths of 50 or 100 mm) following ASTM (2005) D-2922 and ASTM (2010) D-2937 (MD), respectively. Soil samples were collected in 10 kg plastic bags at each excavation level (0.5 m depth intervals) for laboratory testing.

The groundwater table (GWT) was measured in two existing boreholes at 3.1 m depth with the capillary zone met at 2.8 m depth. The GWT was monitored constantly during the period of the field works with no significant variation registered.

The upper soil profile is generally characterized by an approximately 4.7 m thick layer of marine fine to medium sand, overlying a clay layer. The sand is similar to a typical North Sea sand in terms of gradation and mineralogy.

3.1.2. Overview of field test results

3.1.2.1. CPTU results

Figure 4 summarizes the results from the seven CPTUs. The data show a scatter within the circular 10 m diameter testing area. Particle-size distributions (presented later in detail) are more or less constant, indicating homogeneity in material composition. The scatter arises from the varying densities in between thinly laminated microlayers as identified by Fig. 5. The microlayering is considerable and thus, spatial variations of the in situ relative density must be considered within the field-testing area. The layering may likely be an outcome of the depositional environment and the impact of dynamic environmental loading (waves and currents).

3.1.2.2. Unit weight and water content

Unit weight measurements were performed with the ND, and test results proved repeatable above the GWT. MD determinations using push-in cylinders were tried for comparison to the ND results. Although great care was exercised during the MD sampling, the results are more scattered and less reliable than ND measurements, with an operator dependency and the geometrical characteristics of the cylinders (as investigated by using two different cylinder volumes) impacting the results.

Fig. 5. Micro-layering over approximately 4 m depth as observed during excavation works.

Figures 6*a* and 6*b* present water contents and unit weights as measured with the ND and MD methods, respectively. γ and γ_d from MD are consistently lower than the ND values. Figure 6*c* presents a good agreement between dry unit weights of consolidated anisotropic drained triaxial compression (CADC) specimens and the ND values.

Water contents (w) were measured directly by laboratory testing of sampled soil (MD) and indirectly with the ND. Direct measurements were expected to be most representative. The w_{ND} values are consistently lower than the corresponding values obtained from laboratory testing w_{MD}.

3.1.2.3. In situ stress conditions

Measured volumetric water contents ranged from 0.1 m^3/m^3 at 0–2 m depths to 0.2 m^3/m^3 at 3 m depth. Between 0 and 3 m depth, a suction of about 10 $\pm$ 2 kPa was measured using calibrated MP-6 ceramic disks. Measurements of volumetric water content were used for correcting the measured suction with respect to void ratio changes due to sensor installations and the varying degree of saturation with depth. The suction measurements were then used for calculating the vertical effective stresses in the field. Figure 7 shows the total vertical stresses, the suction and pore-water pressures, and the effective vertical stress profiles with depth.

3.2. In situ conditions

Given the scatter in the CPTU profiles in Fig. 4 with e.g., q_c ranging between roughly 10–20 MPa at 1 m depth, the field tests results are further assessed with consideration to two distinct subareas,

Can. Geotech. J. Downloaded from cdnsciencepub.com by NORWEGIAN GEOTECHNICAL INSTITUTE (NGI) on 05/02/23

Fig. 6. Measurements of (*a*) water content, (*b*) unit weight, and (*c*) dry unit weight.

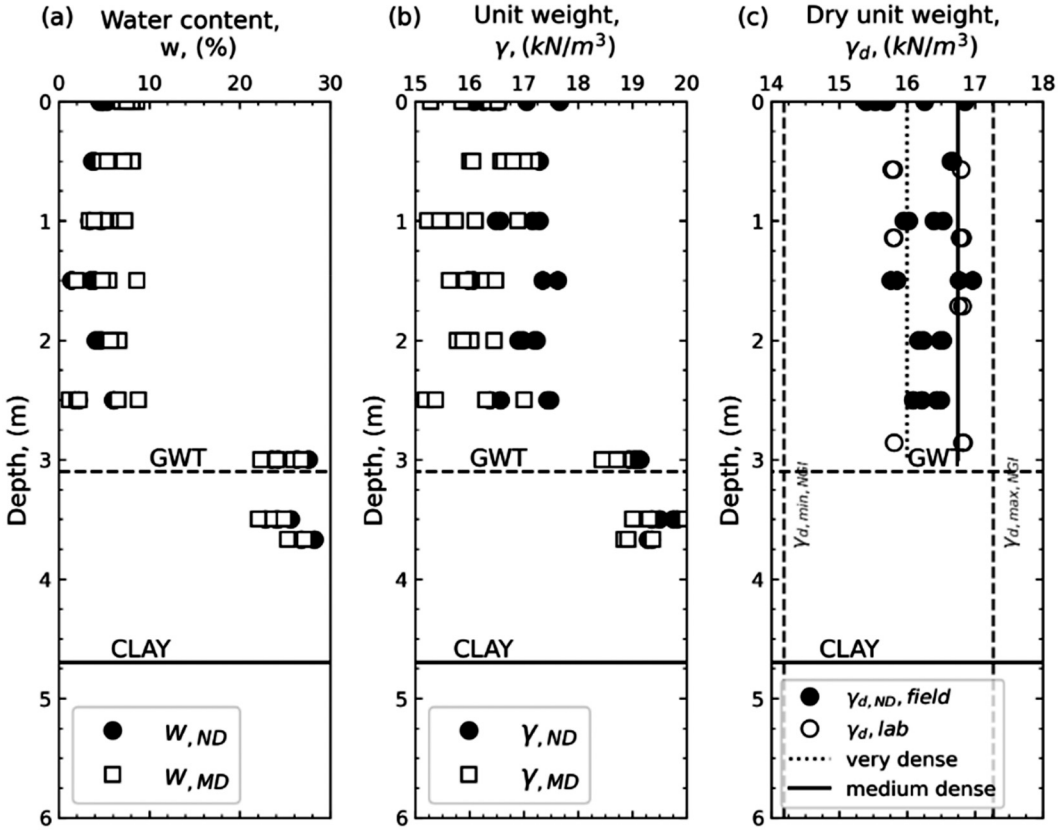

i.e., an area of very dense and medium dense conditions, respectively. CPTU Nos. 03, 04, and 07, representative of the very dense field conditions, and CPTU Nos. 01, 02, 05, 06, representative of the medium dense conditions, are collated in Fig. 8.

Representative profiles in terms of e and D_r are given in Fig. 8 with limiting void ratios determined from measured limiting values of the dry unit weights $\gamma_{d,max}$ and $\gamma_{d,min}$ (see laboratory schedule in Table 1). ND determined unit weights obtained deeper than 2.8 m depth — and thus the void ratios and relative densities derived — are considered unreliable due to workability issues with the ND in wet and saturated conditions due to reflections of the transmitted photons by the radioactive source.

3.2.1. Apparent OCR and K_0

The Cuxhaven site has been excavated by roughly 18 m to current surface level. Hence, an apparent OCR can be assessed for a mechanically OC soil as shown in Figs. 9*a* and 9*c* for overburden heights of 18 ± 2 m for the very dense and medium dense areas, respectively. The apparent OCR is calculated by:

$$\text{OCR} = \sigma'_p/\sigma'_v \quad (4)$$

where σ'_p is the apparent past effective pre-consolidation stress.

The influence of the assumed overburden thickness is more pronounced in the uppermost 2 m compared to larger depths.

Figures 9*b* and 9*d* present the corresponding K_0 distributions as predicted by CPT using the unified approach by Mayne (2009) and Kulhawy and Mayne (1990):

$$\sigma'_p = 0.33(q_t - \sigma_v)^{m'} \quad (5)$$

with

$$K_0 = (1 - \sin\varphi'_{cv})\text{OCR}^{\sin\varphi'_{cv}} \quad (6)$$

where q_t is the corrected cone resistance, σ_v is the vertical total stress, m' is a fitting exponent equal to $m' \approx 0.72$ for clean quartz and silica sands, and φ'_{cv} is the measured constant volume friction angle as suggested for denser sands by Lee et al. (2013).

The OCR profile calculated based on Mayne (2009) using eqs. 4 and 5 is observed to fit the apparent OCR due to removal of 18 ± 2 m overburden.

4. Laboratory testing

4.1. Testing programme

Index and advanced laboratory tests (oedometer, triaxial and bender elements) were performed, see Table 1 and Quinteros et al. (2017) for additional details. Sieve analyses were performed on samples retrieved at each excavation level. A comparison of the grain-size distributions allowed for mixing sample material from all depths to one single representative batch used for the laboratory testing, cf. Fig. 10.

Several methods were applied for determining the minimum and maximum dry densities due to the particular method dependency on their results (Blaker et al. 2015; Lunne et al. 2019). The DIN 18126 (DIN 1996) two-prong impactor method along with Norwegian Geotechnical Institute (NGI) and Geolabs proprietary methods were tried and compared for the maximum dry density. Results of NGI's proprietary procedures (described in Lunne et al. 2019) are taken further because they are evaluated as most reliable and in line with previously experienced values for similar sands.

4.2. Triaxial testing

CADC tests were conducted for informing on the stress–strain–strength response of a sand specimen representative of

Can. Geotech. J. Downloaded from cdnsciencepub.com by NORWEGIAN GEOTECHNICAL INSTITUTE (NGI) on 05/02/23

Fig. 7. Measurements of suction: (*a*) total vertical stress, (*b*) suction and pore–water pressure, and (*c*) effective vertical stress.

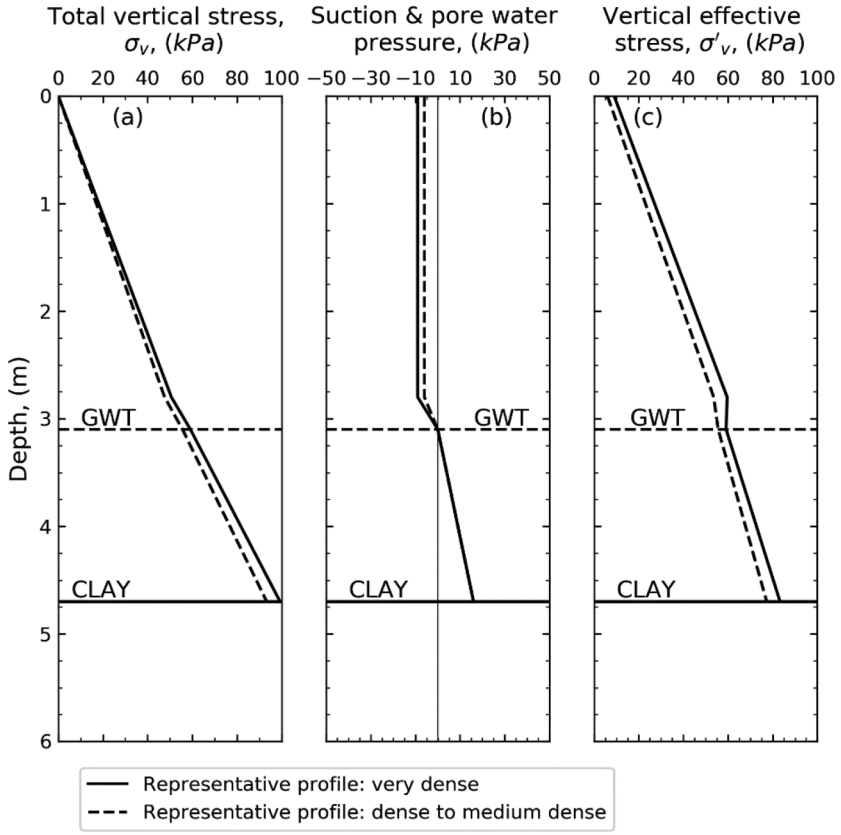

OC conditions at low stress levels as well as for calibration purposes of the constitutive model for numerical analyses. Specimens were reconstituted by moist tamping following Ladd's undercompaction method, using an undercompaction factor of 4% and an initial water content of 4%, in six soil layers, and consolidated to target in situ relative densities.

Eighteen CADC tests were performed with different combinations of relative density (D_r values of 57% and 87%), effective vertical stress (σ'_{vc} values of 10, 20, and 50 kPa) and stress anisotropy (K_0 values of 1.0 and 2.0). Tests performed at higher vertical effective stresses, i.e., 200 kPa, were performed covering a larger stress range for comparison with existing databases. A detailed outline of the testing program, specimen reconstitution, and testing procedures as well as all results are presented in Quinteros et al. (2017).

4.2.1. Comparisons to existing databases

Figure 11 compares the measured effective peak friction angles (φ'_p) to the predicted trend from Bolton's dilatancy theory (Bolton 1986). The friction angles decrease with decreasing relative density and increasing effective mean stresses. Although Bolton's database of tests on 16 sands was developed for stresses higher than 150 kPa, the theory appears to capture the peak angles also at stress levels down to 10 kPa with an accuracy of ±2°. The mobilized effective peak friction angles present a considerable increase in strength ($\Delta\varphi'_p > 10°$) in comparison to the results of the CADC database presented by Emerson et al. (2008) on NC siliceous Hostun and Fontainebleau sands.

5. Numerical analyses

An FE study was performed to gain insight into the mechanisms of a penetrating cone at shallow depths by investigating the soil response and development of failure mechanisms. This study uses the arbitrary Lagrangian–Eulerian (ALE) and the coupled Eulerian–Lagrangian (CEL) methods, in combination with advanced hypoplastic constitutive models (Masin 2011), in the software package Abaqus to simulate the entire penetration process of a CPT in NC and OC sands, respectively. CEL is applied for more advanced large deformation analysis capabilities, whereas the ALE is computationally more efficient for investigating the K_0 effects.

The FE models and corresponding material and model parameters have been calibrated against the field and laboratory test results. The model performance has been validated against CC test results and acknowledged empirical correlations. Sensitivity studies have informed on the choice of constitutive model, discretization, applied rate of cone penetration, and cone–soil interface roughness. Several analyses have been performed with the calibrated and validated model to investigate the effects of D_r, K_0, and stress levels on the cone penetration response. Details of the model, approach, boundary conditions, validations, parameters, analyses, and results are presented in Engin et al. (2018). An overview of the main findings is given herein with focus on the failure mechanisms.

5.1. Results

5.1.1. Failure mechanisms and evaluation of critical depth

Figures 12 and 13 present the development of failure mechanisms from the cone penetrating the soil surface to greater depths as investigated by the ALE modelling for $D_r = 0.65$ and $D_r = 0.85$, respectively, with consideration to the effect of a constant and varying K_0 with depth (NC versus OC response).

The cone resistance and normalized cone resistance versus depth reveal different failure mechanisms by the shape and changing curvatures of the distributions. The response presents an uppermost surficial failure (concave part, up to roughly 0.5 m

Fig. 8. q_c, e, and D_r measured and derived from field testing for (*a*–*c*) very dense and (*d*–*f*) medium dense areas.

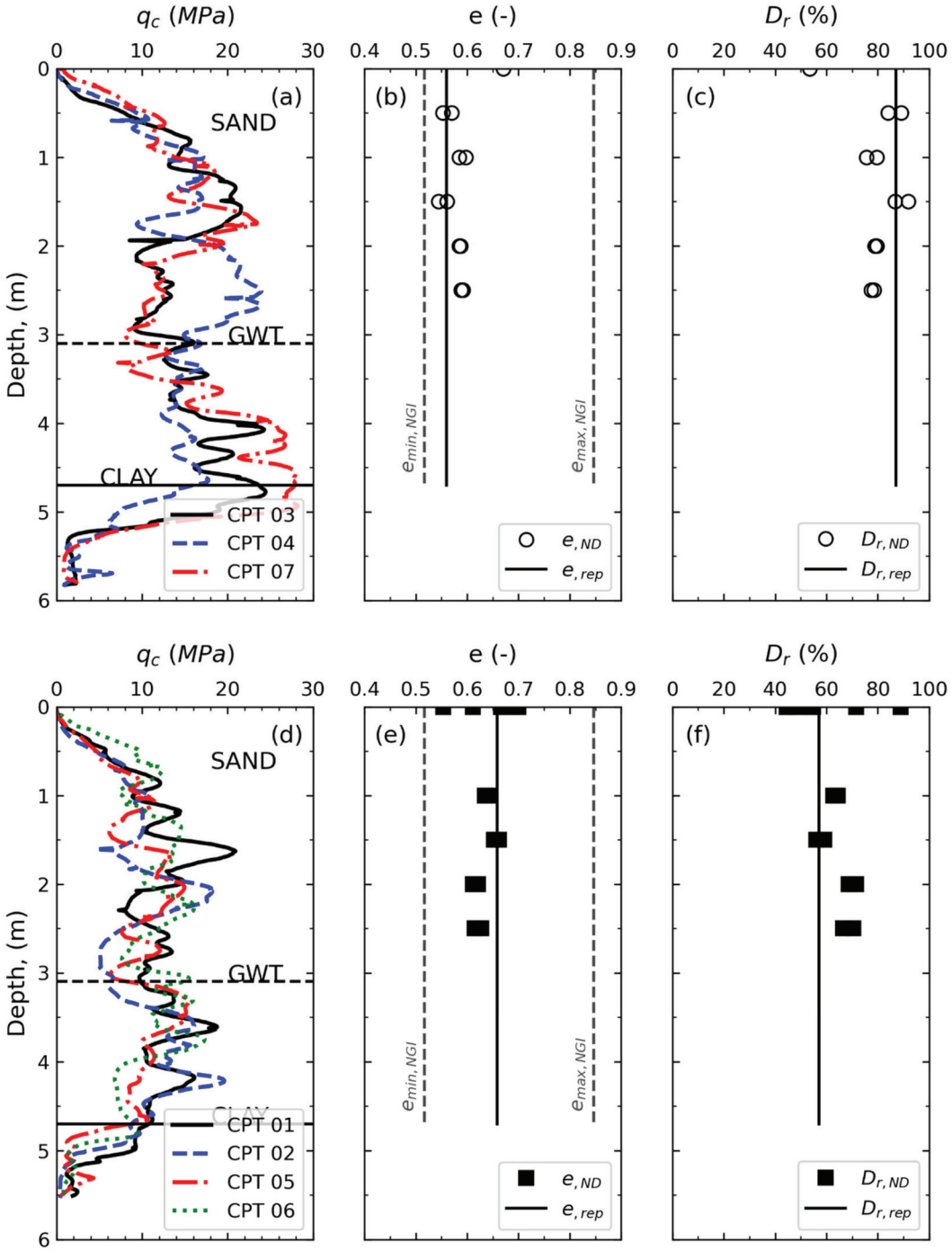

depth) developing into a transition zone (linear to a convex shape, at the depth range ~0.5–1 m) towards the deep failure (convex part), in line with the general observations by Emerson et al. (2008) and Senders (2010).

Figure 12 also indicates that the critical depth may be met at shallower depths for a higher density, whereas a varying and larger K_0 may involve a critical depth at greater depths. Deep failure mechanisms (full flow) dominate below the critical depth, and the depth for reaching a quasi-stationary state q_{st} depends on the fabric and structure of the sand as well as the stress conditions.

Figure 13 presents the velocity fields at selected depths (identified in Fig. 12) for more information about the development of failure surfaces.

The mobilized zones around the penetrating cone are found with a radial extent of ~4.5–6 cone diameters in the cases considered, and the impacted zone below the cone tip is roughly 0.5–2.5 cone diameters. K_0 appears to affect the shape of the extension zone at surficial depth and to force the failure zone to expand radially as the confinement towards the tip increases for the depth dependent $K_0 = K_0(z)$ case.

Can. Geotech. J. Downloaded from cdnsciencepub.com by NORWEGIAN GEOTECHNICAL INSTITUTE (NGI) on 05/02/23

Can. Geotech. J. Downloaded from cdnsciencepub.com by NORWEGIAN GEOTECHNICAL INSTITUTE (NGI) on 05/02/23

Table 1. Laboratory testing programme.

Test type	Test description	Symbol	Unit	No. of tests	Value/result
Index	Grain-size distribution, wet sieving	D_{10}	mm	10	0.10 ± 0.02
		D_{60}	mm	10	0.22 ± 0.02
		C_U	—	10	2.1 ± 0.3
		C_C	—	10	1.1 ± 0.1
	Water content above GWT	$w_{aboveGWT}$	%	9	6 ± 2
	Water content below GWT	$w_{belowGWT}$	%	9	25 ± 2
	Unit weight of solid particles	γ_s	kN/m^3	4	26.2 ± 0.2
	Maximum unit weight	$\gamma_{d,max}$	kN/m^3	4	17.27 ± 0.04
	Minimum unit weight	$\gamma_{d,min}$	kN/m^3	4	14.19 ± 0.01
	Mineralogy X-ray diffraction	XRD	—	2	92.5% uartz 4.5% alkali-feldspar 3% plagioclase
	Scanning-electro-micrograph; particle shape	SEM	—	1	59.6% subrounded 26.4% rounded 12.4% subangular
	Particle roundness	R	—	1	0.78 ± 0.05
	Particle sphericity	S	—	1	0.90 ± 0.02
	Particle regularity	ρ	—	1	0.82 ± 0.02
	Friction angle of repose*	φ'_{rep}	°	4	30 ± 1
Advanced	Oedometer, constant rate of strain	CRS	—	2	Quinteros et al. (2017)
	Triaxial, consolidated anisotropic drained compression	CADC	—	18	See Section 4.1 and Quinteros et al. (2017)

*Friction angle of repose after Santamarina and Cho (2001).

Fig. 9. Apparent OCR and K_0 profiles for Cuxhaven for (*a*, *b*) very dense and (*c*, *d*) medium dense areas for 16–20 m overburden. Note that $K_0 \leq K_P$.

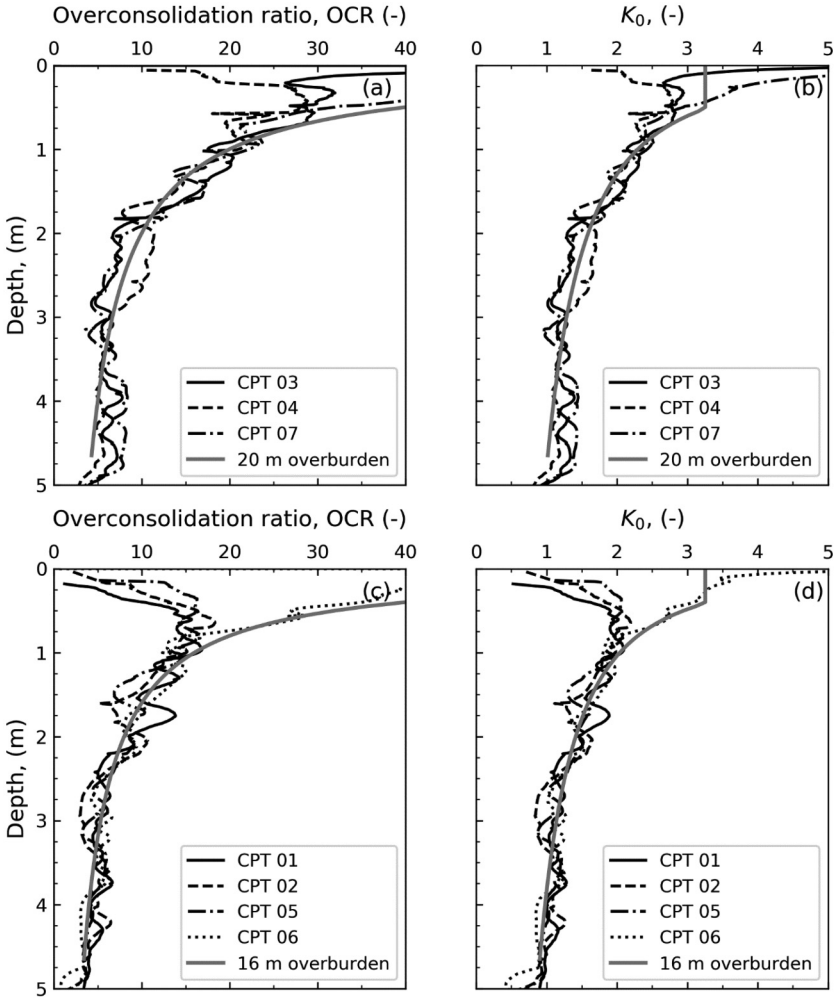

Can. Geotech. J. Downloaded from cdnsciencepub.com by NORWEGIAN GEOTECHNICAL INSTITUTE (NGI) on 05/02/23

Fig. 10. Grain–size distributions of samples and batch prepared for testing (an SEM is included).

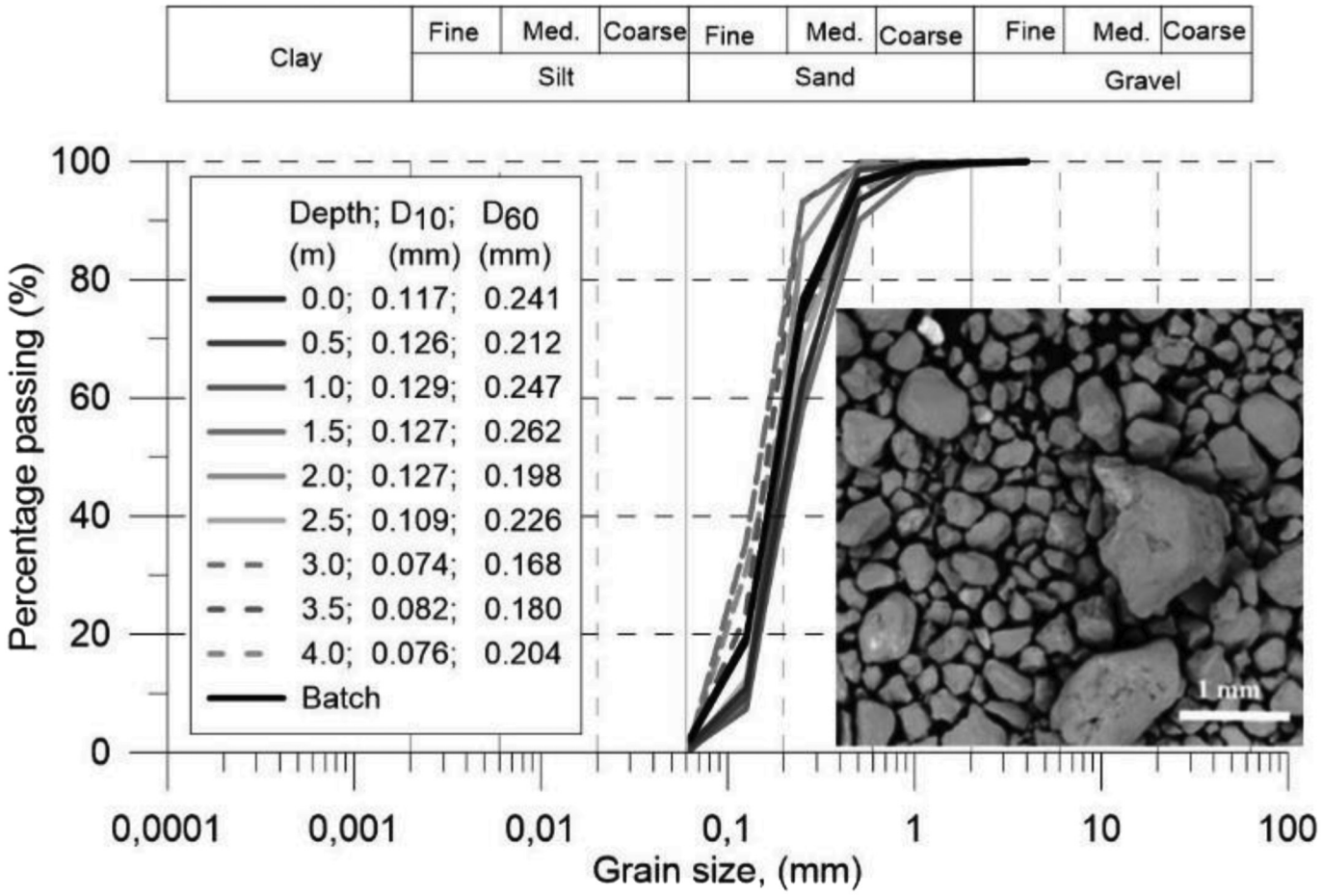

Fig. 11. Effective peak friction angles compared to predictions using Bolton's dilatancy theory.

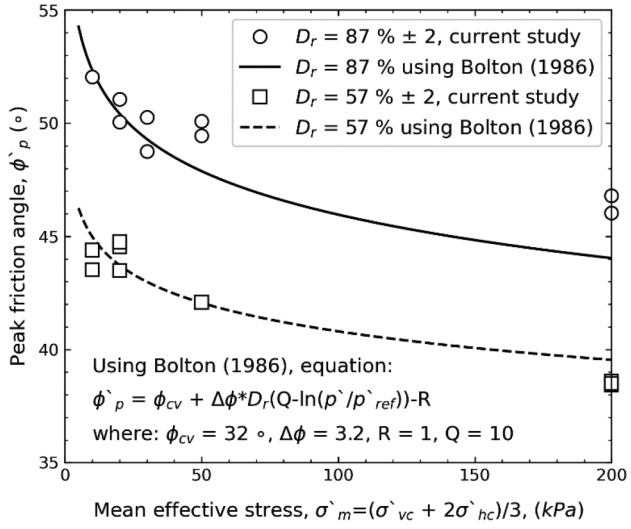

5.1.2. Effect of density and OCR/K_0

Effects of D_r and K_0 on the cone resistance as predicted by CEL and ALE analyses are summarized and compared in Fig. 14. D_r has a more pronounced impact on the cone resistance and the rate of the increasing q_c compared to K_0. However, an increasing K_0 value returns a higher cone resistance as well, especially when K_0 is allowed to vary with depth in accordance with the OCR distribution, i.e., $K_0 = K_0(z)$. The effect is most clear for penetrations deeper than ~1 m. The ALE results, although restricted to $K_0 \leq K_P$ (where K_P is the coefficient of passive earth pressure), identify the effects of K_0 more clearly compared to the CEL results, given CEL is restrained to a constant and limiting K_0 value of 1.0.

Figure 15 compares the CEL and ALE cone resistances with the correlations by Jamiolkowski et al. (2003), Emerson et al. (2008), and Senders (2010). The response in the surficial and transitional zones do not compare well with the correlation by Jamiolkowski et al. (2003), although the cone resistances converge at greater depths for constant values of $K_0 \leq 1.0$.

Furthermore, the effect of an increased and varying K_0 is not adequately captured by any of the existing empirical models at surficial and transitional depths, although both Senders (2010) and Emerson et al. (2008) capture the concave curvature of the surficial part. The critical depths predicted by FE analyses appear to be shallower than proposed by both Senders (2010) and Emerson et al. (2008).

Regarding the bold solid red curves in Fig. 15 none of the existing empirical correlations appear to be able to capture the q_c distribution at greater depths as well in OC sands with K_0 values varying with depth and increasing beyond $K_0 = 1.0$, where the cone resistance consistently is underpredicted for both densities investigated.

6. Revisiting CPT correlations to relative density

D_r obtained according to Jamiolkowski et al. (2003), cf. eq. 1, and Mayne (2009), cf. eq. 3, adopting $K_0 = 1$ as usually done in practice for

Can. Geotech. J. Downloaded from cdnsciencepub.com by NORWEGIAN GEOTECHNICAL INSTITUTE (NGI) on 05/02/23

Fig. 12. Cone resistance and normalized cone resistances versus depth for D_r = 65% and D_r = 85% for K_0 = 0.415 and $K_0 = K_0(z) \leq K_P$. Stars mark selected depths for presentation of velocity fields.

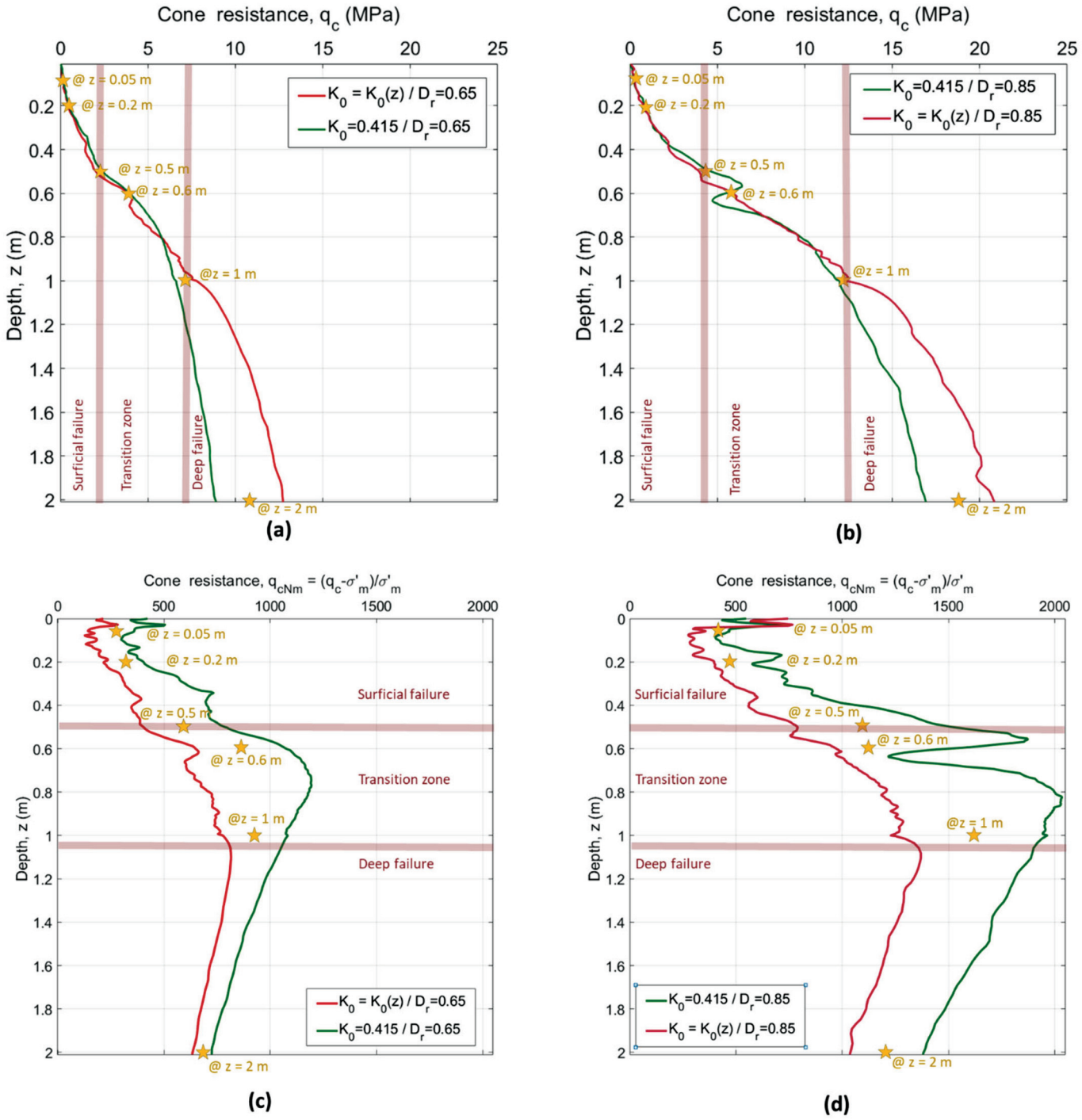

OC sands, is in Figs. 16*a* and 16*b* compared to the Cuxhaven field measurements for a representative CPT for the medium dense–dense (CPTU No. 02) and very dense (CPTU No. 04) parts of the site, respectively. The expression by Jamiolkowski et al. (2003) is corrected for saturation effects below 3 m depth, employing eq. 2.

The impact of the choice of a depth-constant K_0 value on the estimated D_r with Jamiolkowski et al. (2003) is presented in Figs. 16*c* and 16*d* with 0.5, 1.0, and 1.5.

Both empirical correlations by Jamiolkowski et al. (2003) and Mayne (2009) return comparable D_r profiles (expected as the formulations are based on the same CC data). Although the methods are not strictly applicable for shallow depths, they estimate D_r with a variation of ±10 percent-points. However, the choice of different values of K_0 of 0.5, 1.0, and 1.5 introduces a variation of D_r of up to roughly ±20 percent-points. This supports the conclusions of the numerical modelling, that adopting the right value of K_0 appears to be more important for the D_r estimate at shallow depths than the choice of the prediction formulation itself.

A comparison of the CPT correlations by Jamiolkowski et al. (2003), Emerson et al. (2008), and Senders (2010) using K_0 = 1

Can. Geotech. J. Downloaded from cdnsciencepub.com by NORWEGIAN GEOTECHNICAL INSTITUTE (NGI) on 05/02/23

Fig. 13. Development of failure mechanisms (velocity fields) for D_r = 65% and D_r = 85% as investigated for $K_0 = K_0(z) \leq K_P$ and K_0 = 0.415.

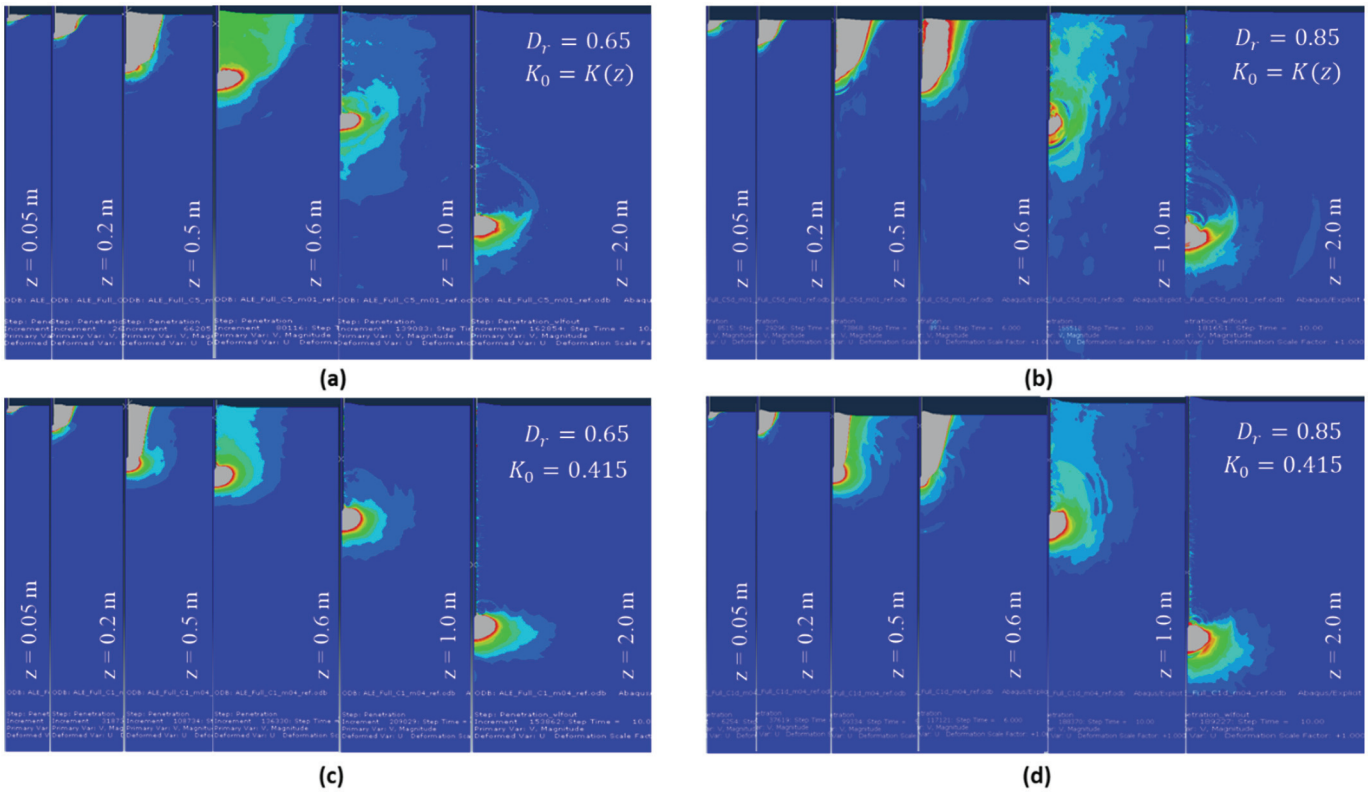

Fig. 14. Effects of D_r and K_0 on cone penetration resistance calculated from (*a*) CEL analyses. Note that K_0 is constant and limited to $K_0 \leq$ 1.0 and (*b*) ALE analyses, where K_0 is limited to $K_0 \leq K_P$.

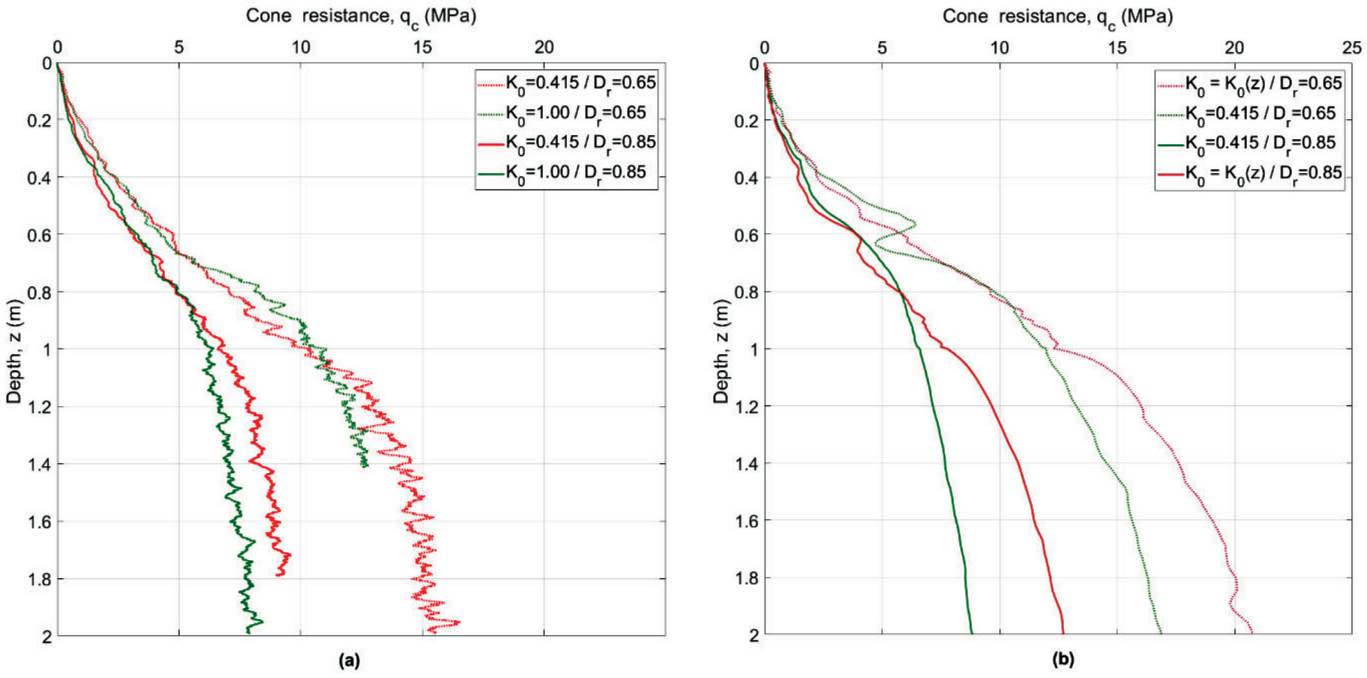

is shown in Fig. 17. Emerson et al. (2008) suggested the use of a K value different to K_0, where K changes with the degree of saturation (ranging between 0.8 for dry and 1.3 for saturated sand). However, to ease direct comparison is the approach by Emerson et al. (2008) presented with $K = K_0 = 1.0$ as well. D_r is iterated in terms of predicted q_c versus depth as originally presented in Emerson et al. (2008) and Senders (2010). Emerson et al. (2008) appears to capture the curvature of the q_c distribution for both the medium dense–dense and very dense conditions, whereas Senders (2010) underestimates D_r in the uppermost couple of

Can. Geotech. J. Downloaded from cdnsciencepub.com by NORWEGIAN GEOTECHNICAL INSTITUTE (NGI) on 05/02/23

Fig. 15. Comparison of FE results with empirical predictions (*a*) CEL analyses for D_r = 0.65, (*b*) CEL analyses for D_r = 0.85, (*c*) ALE analyses for D_r = 0.65, and (*d*) ALE analyses for D_r = 0.85.

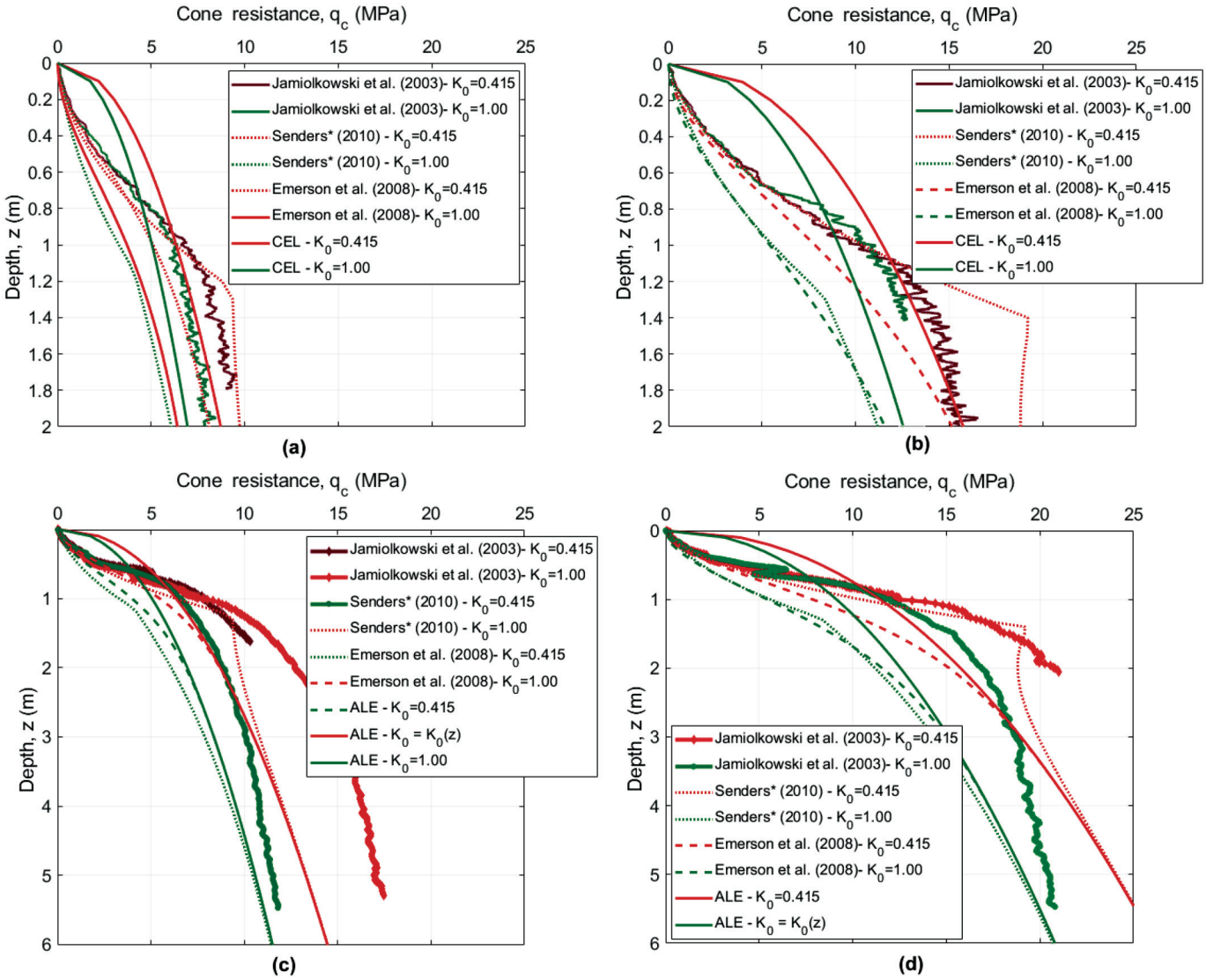

metres. Jamiolkowski et al. (2003) provides a reasonable estimate of D_r in the upper metres, although not capturing the concave surficial shape and still with a considerable underestimation between 0.5–1.5 m depth.

The nominal average relative densities for the very dense and the medium dense areas are roughly 87% and 57%, respectively, with natural variations of roughly ±10 percent-points. Figure 18 presents the sensitivity of the iterated D_r using Emerson et al. (2008) compared to the field results. Figure 18*a* illustrates that the q_{st} iterates to a higher value than actually measured for Emerson et al. (2008) to converge for the very dense conditions. This is due to the fact that the method is challenged by modelling the change between shallow and deep responses. However, Emerson et al. (2008) nicely captures the results obtained in the medium dense conditions, cf. Fig. 18*b*.

It can thus be summarized that

- Comparable values of D_r are obtained from the empirical correlations by Jamiolkowski et al. (2003) and Mayne (2009) using a constant value of K_0 = 1.0. Both predictions appear to return reasonable estimates of D_r, also at stress levels below 50 kPa.
- The mean effective stresses, and thus the selected profile of K_0, are found to significantly impact the D_r estimate, and it appears that a variation of the K_0 profile with depth is needed for appropriately capturing the measured q_c distributions in OC sands.
- D_r predictions using the existing shallow CPT methods (for constant K_0 values), such as Emerson et al. (2008) and Senders (2010), return reasonable results for the medium dense sand in the OC case, whereas the predicted D_r values appear to be more questionable for the very dense conditions. Emerson et al. (2008) predictions appear to perform more reasonably than those of Senders (2010).

7. Recommended approach for interpretation of relative density

7.1. Summary of observations

The following observations and learnings as gained from the field and laboratory testing as well as the numerical analyses are key for supporting the recommendations.

The in situ testing provides

- A suite of natural CPT q_c distributions of aged, OC medium dense and very dense sand similar to typical North Sea conditions,

Can. Geotech. J. Downloaded from cdnsciencepub.com by NORWEGIAN GEOTECHNICAL INSTITUTE (NGI) on 05/02/23

Fig. 16. Comparisons of D_r predictions for (*a*) CPTU 04 representing very dense site and (*b*) CPTU 02 representing medium dense site; (*c*) and (*d*) investigate impact of K_0 for values of 0.5, 1.0, and 1.5.

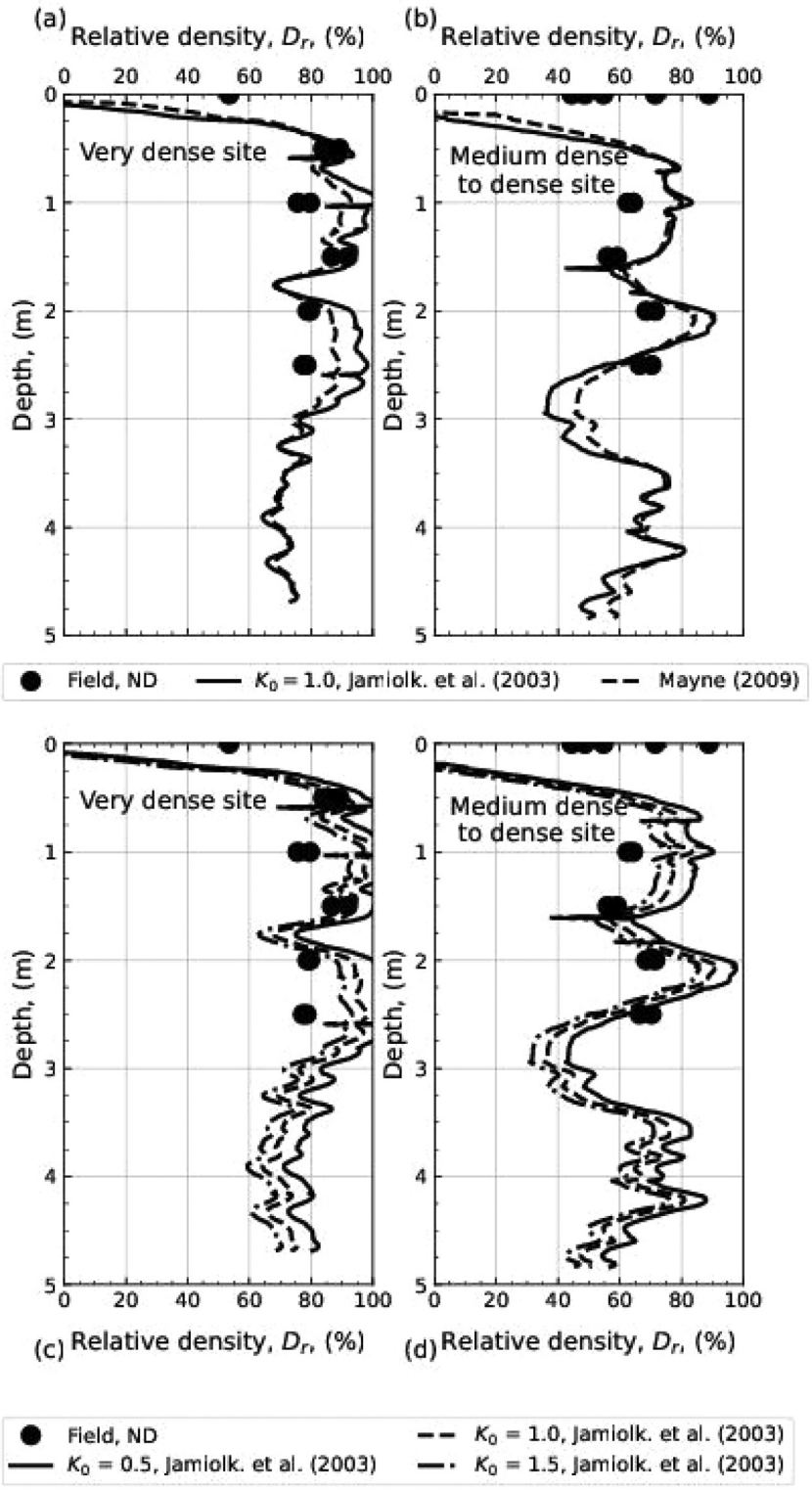

allowing for a comparison with existing q_c distributions of NC sands, both natural and as reconstituted in CCs.

- Although slightly scattered, density measurements with the ND are found applicable for direct comparison with laboratory density measurements and appear to be representative for the in situ conditions.
- A thorough characterization of in situ conditions, including the determination of stress conditions (the apparent OCR and K_0 profiles).
- Confirmation that an aged OC sand indeed returns highly increased q_c values at shallow depths compared to an unaged NC sand, in line with observations from offshore conditions.

Can. Geotech. J. Downloaded from cdnsciencepub.com by NORWEGIAN GEOTECHNICAL INSTITUTE (NGI) on 05/02/23

Fig. 17. Comparison of CPT predictions with measurements obtained in OC sands at shallow depths at (*a*) very dense area and (*b*) medium dense area. $K = K_0 = 1.0$.

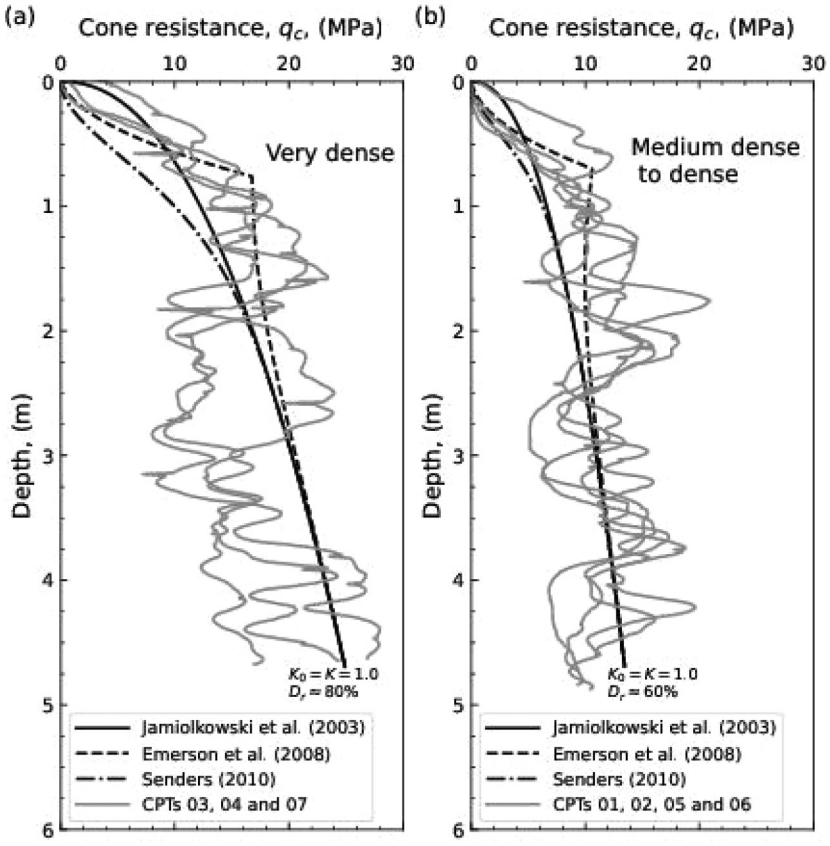

- Acknowledgement of the uncertainties related to a Cuxhaven sand unit, which is very homogeneous in material composition, but inhomogeneous due to micro-layering (spatially varying relative densities).

The laboratory testing provides

- A detailed characterization of the Cuxhaven sand unit, including mineralogy and particle characterization, as well as stress–strain and stress–strength responses required for calibration of the constitutive modelling in the numerical analyses.
- CADC results obtained at low stress levels support the observation of the highly increasing cone resistances measured at shallow depths in OC sands.
- Acknowledgement that the database of laboratory testing indicates that the formulation by Emerson et al. (2008) appears to underestimate the strength of a typical very dense OC North Sea sand.

The numerical analyses provide

- An understanding of the failure mechanisms of a penetrating cone in medium dense and very dense conditions, identifying responses of surficial and deep penetration (full flow below critical depth) through a transition zone.
- Appreciation that a very dense sand appears to mobilize the failure mechanism at shallower depth compared to a medium dense sand, and that a larger and varying K_0 with depth returns an increasing critical depth.
- Understanding that highly varying OCR and K_0 distributions in the uppermost metres indeed involve rapidly increasing q_c values in OC sand units as measured in the field.

A review of existing empirical CPT correlations for relative density concludes that the existing formulations by Jamiolkowski et al. (2003) and Mayne (2009) do not differ from each other. To model the CPT response of an OC sand, it is more important to capture the mean effective stress, i.e., include the appropriate effects of a varying OCR and K_0 profile, in the uppermost metres than trying to select the most appropriate of the existing formulations. The existing correlations appear to embrace also the response of an OC sand, if and when K_0 is modelled appropriately.

7.2. Recommendation for estimating relative density from CPT

Typical dense OC marine and offshore sand units show logarithmically decreasing values of OCR and K_0 with depth (see Fig. 9). Thus, a practical stepwise recommendation is given for predicting D_r in the uppermost metres as well as at greater depths of both OC and NC sands from CPT with due consideration to varying OCR and K_0 profiles.

Step 1

Estimate the distribution of the apparent OCR using, for instance Mayne (2009), where the apparent pre-consolidation pressure at each depth *i*, $\sigma'_{p,i}$, is determined from $\sigma'_{p,i} = 0.33(q_{t,i} - \sigma_{v,i})^{m'}$, cf. eq. 5, and $OCR_i = \dfrac{\sigma'_{p,i}}{\sigma'_{v,i}}$, cf. eq. 4, with fitting exponent $m' \approx 0.72$ for clean quartz to silica sand (as recommended by Mayne 2009).

Can. Geotech. J. Downloaded from cdnsciencepub.com by NORWEGIAN GEOTECHNICAL INSTITUTE (NGI) on 05/02/23

Fig. 18. Variations of D_r as exemplified by Emerson et al. (2008) in comparison with measurements obtained in OC sands at shallow depths for: (*a*) very dense area and (*b*) medium dense area. $K = K_0 = 1.0$.

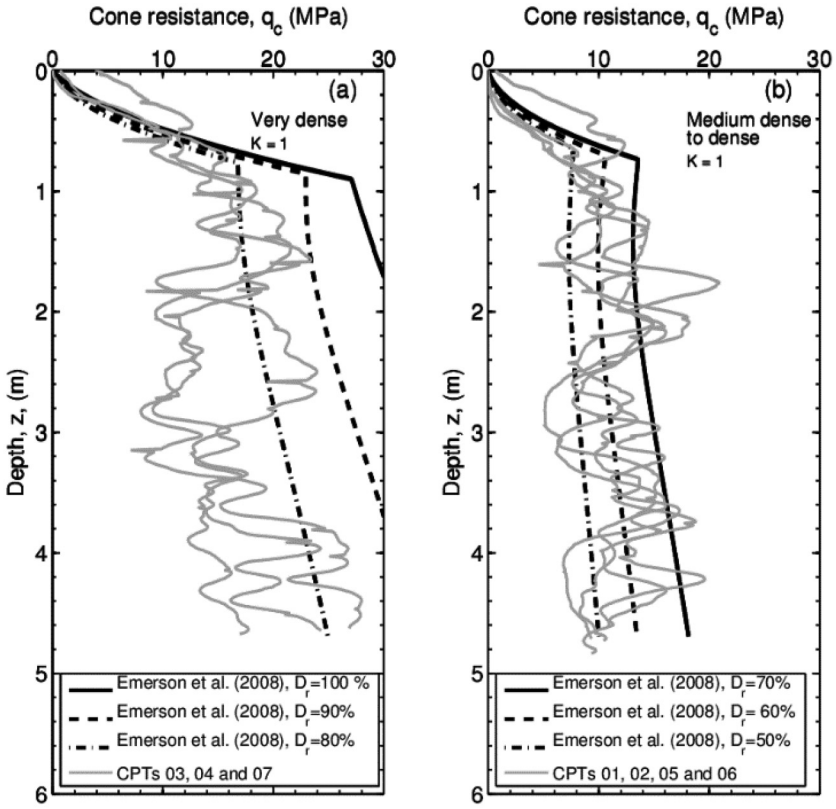

Fig. 19. (*a*) Impact of constant and varying K_0 values on q_c distributions at shallow depths, (*b*) comparison of correlations discussed and recommendations given with representative field measurements.

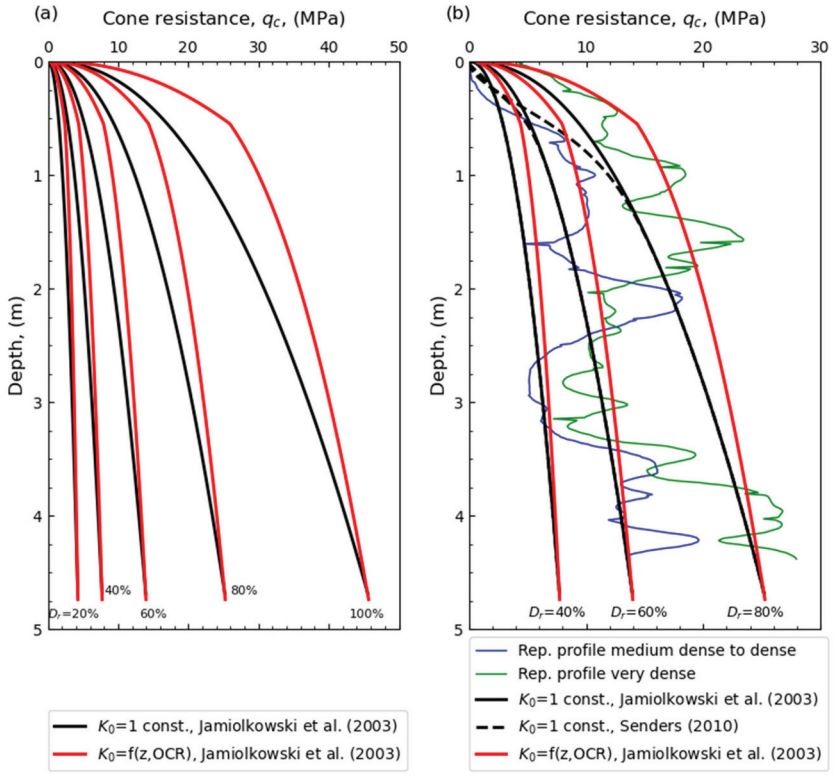

Can. Geotech. J. Downloaded from cdnsciencepub.com by NORWEGIAN GEOTECHNICAL INSTITUTE (NGI) on 05/02/23

Fig. 20. CPT correlations to relative density exemplified for three representative North Sea CPTs: (*a*–*d*) D_r = 115%; (*e*–*h*) D_r = 80%; (*i*–*l*) D_r = 50%. $K_0 \leq K_P = 3.5$.

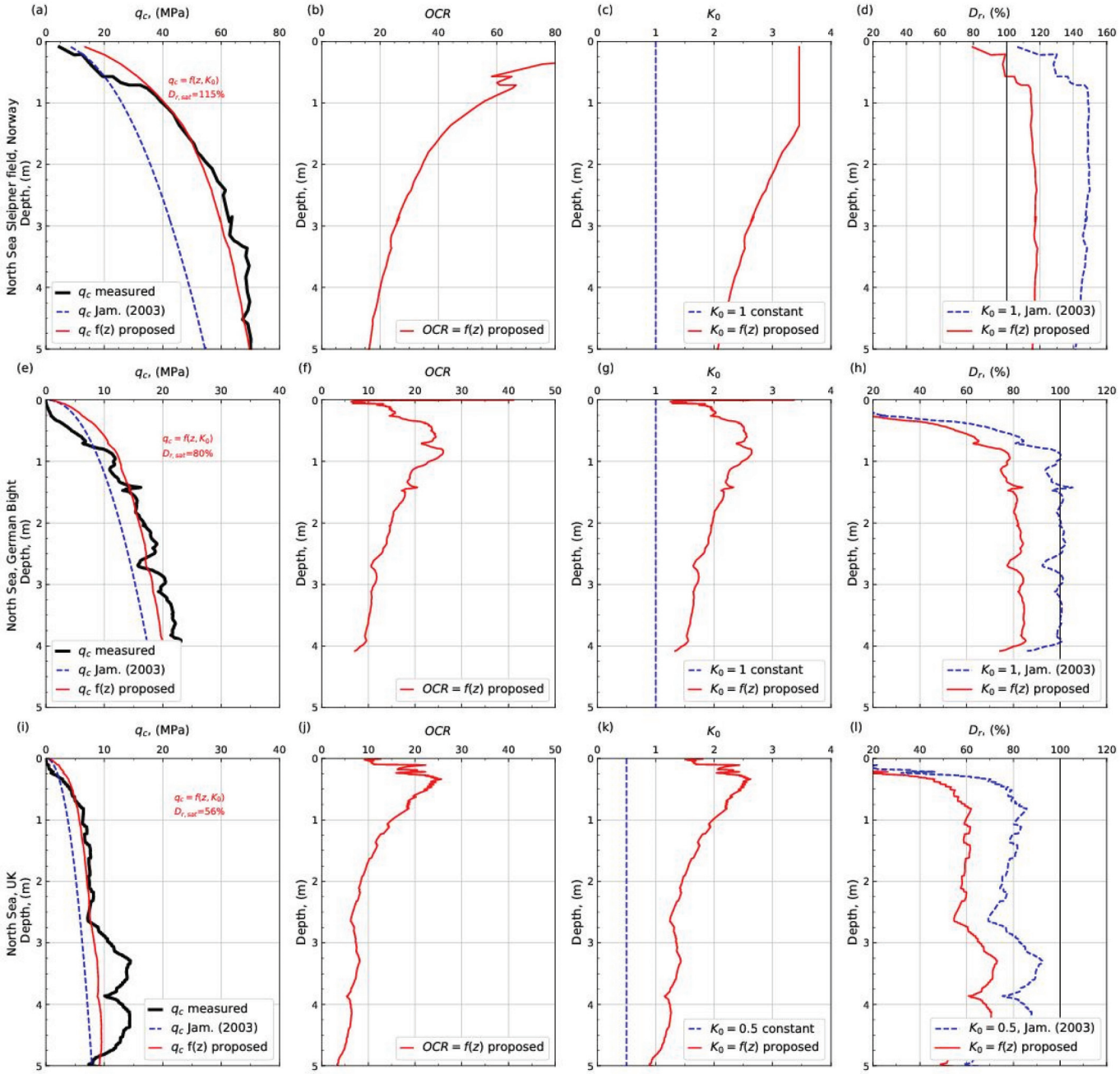

Step 2

Apply a measured or estimated constant volume friction angle φ'_{cv} for determining $K_{0,i}$, using e.g., $K_{0,i} = (1 - \sin\varphi'_{cv})\mathrm{OCR}_i^{\sin\varphi'_{cv}}$, cf. eq. 6, with reference to Kulhawy and Mayne (1990) and Lee et al. (2013). With obtained $K_{0,i}$ mean effective stresses can now be determined as $\sigma'_{m,i} = \frac{\sigma'_{v,i}}{3}(1 + 2K_{0,i})$. A maximum value of $K_0 = K_P$ = 3.5 is applied.

Step 3

Once the $\sigma'_{m,i}$ profile is obtained, Jamiolkowski et al. (2003), cf. eq. 1, is applied for determining D_r from the measured cone resistance q_c:

$$q_{c,i} = 24.94\left(\frac{\sigma'_{m,i}}{p_a}\right)^{0.46} e^{2.96D_{r,i}} \quad \text{or} \quad D_{r,i} = \frac{1}{2.96}\ln\frac{q_{c,i}}{24.94\left(\sigma'_{m,i}/p_a\right)^{0.46}}$$

7.3. Examples of application

Figure 19*a* exemplifies the impact of varying K_0 and OCR on the q_c distributions based on conditions determined for the Cuxhaven site, whereas Fig. 19*b* compares the measured and calculated q_c profiles, based on the recommendations.

Acknowledging the inhomogeneity of the representative cone resistance profiles obtained in Cuxhaven, Jamiolkowski et al. (2003)

Can. Geotech. J. Downloaded from cdnsciencepub.com by NORWEGIAN GEOTECHNICAL INSTITUTE (NGI) on 05/02/23

using K_0 = 1 suggests lower bounds of the cone resistances measured. In contrast, the impact of a varying K_0 value with depth on the shape of q_c is clearly demonstrated, particularly for the very dense profile where the average cone resistance is better captured in the uppermost metres. The surficial concave shape as predicted by Senders (2010) captures the measured uppermost shape of the representative medium dense profile.

Figure 20 presents cone resistances measured at three different North Sea sand sites and further examples on the use of the proposed approach for interpreting D_r. The first q_c profile is obtained in a thick, homogeneous, very dense and highly OC sand deposit found at the Sleipner site offshore Norway (Lunne et al. 1997). The second profile is from a dense–very dense OC sand unit at an Ørsted offshore wind farm site in the German Bight, and the third profile is from a medium dense and slightly OC sand layer at an offshore wind farm site in the British sector of the North Sea.

The recommended approach results in a predicted distribution of the cone resistance, which satisfactorily captures the measured distribution in these very dense and highly OC sand units. Figures 20*a*–20*d* present an iterated relative density value above 100%, which however is commonly observed for offshore conditions.

The observed increase of q_c right below the ground surface is captured. Jamiolkowski et al. (2003) using a constant K_0 = 1.0 underpredicts the actual cone resistances. The highly varying surficial response (below 0.6 m depth) as often encountered in the offshore profiles will often reflect the presence of a thin younger/more recent mobile sand unit or mud covering the seafloor.

Figures 20*e*–20*h* and 20*i*–20*l* exemplify similar conclusions for a slightly less homogeneous dense to very dense sand layer and a medium dense and only slightly OC sand, respectively. Also, for the less dense unit, which may even be NC considering separately the potential effect of increased yield stress due to the dynamic environment in the uppermost metres, the proposed approach allows for a more adequate prediction.

8. Conclusions

A three-legged study comprising of comprehensive field testing for measuring reliable in situ density and relative density, supported by laboratory testing and numerical analyses, has been conducted for investigating the impact of overconsolidation and stress conditions on the CPT-derived relative density of medium dense to very dense sands at shallow depths.

The studies show that capturing the mean effective stresses is indeed very important for modelling the response of a penetrating cone at shallow depths as measured at many offshore sites in the North Sea. Examples and comparisons show that although existing correlations between CPT and relative density as proposed by Jamiolkowski et al. (2003) and Mayne (2009) do not explicitly account for the effect of low stress levels, they are able to capture the measured response obtained at shallow depths, when the varying apparent OCR and K_0 profiles are properly accounted for. On the back of this conclusion, a step-wise approach is suggested for providing a consistent set of parameters, linking the CPT parameters to stress conditions and relative density. Examples of application to CPT profiles as typically obtained in the North Sea prove that the shallow depth response is better captured with due consideration to the mean stress conditions.

Acknowledgements

The support of the Norwegian Geotechnical Institute (NGI) and the Norwegian Research Council is acknowledged with gratitude. Special thanks to J.B. Clausen, S. Bøtker-Rasmussen, and B.A.S. Mousing from Geo for performing the field works and exercising the greatest care during execution. Further special thanks to NGI colleagues, H.D.V. Khoa, H.P. Jostad, D.A. Kort, and H. Sturm for their significant contributions to the numerical part of this study. Many thanks are also extended to former and current Ørsted colleagues R.B. Pedersen and A.H. Augustesen, respectively, for their valuable contributions during the project and review phases.

References

ASTM. 2005. Standard test methods for density of soil and soil-aggregate in place by nuclear methods (shallow depth). ASTM D2922. ASTM International, West Conshohocken, PA.

ASTM. 2010. Standard test method for density of soil in place by the drive-cylinder method. ASTM D2937. ASTM International, West Conshohocken, PA.

Baldi, G., Bruzzi, D., Superbo, S., Battaglio, M., and Jamiolkowski, M. 1986. Interpretation of CPTs and CPTUs; 2nd part: drained penetration of sands. *In* Proceedings of the Fourth International Geotechnical Seminar, Singapore. pp. 143–156

Biarez, J., and Grésillon, J.M. 1972. Essais et suggestions pour le calcul de la force portante des pieux en milieu pulvérulent. Géotechnique, **22**(3): 433–450. doi:10.1680/geot.1972.22.3.433.

Blaker, Ø., Lunne, T., Vestgården, T., Krogh, L., Thomsen, N.V., Powell, J.J.M., and Wallace, C.F. 2015. Method dependency for determining maximum and minimum dry unit weights of sands. *In* Proceedings of the the 3rd International Symposium on Frontiers in Offshore Geotechnics (ISFOG), Taylor & Francis Group, Oslo. pp. 1159–1166.

Bolton, M.D. 1986. The strength and dilatancy of sands. Géotechnique, **36**(1): 65–78. doi:10.1680/geot.1986.36.1.65.

DIN. 1996. Soil investigation and testing – Determination of minimum and maximum dry densities of non-cohesive soil. DIN 18126. German Institute for Standardisation (DIN).

Emerson, M. 2005. Corrélations entre données géotechniques et géophysiques à faible profondeur dans des sables. Ph.D. thesis, Institut National Polytechnique de Grenoble.

Emerson, M., Foray, P., Puech, A., and Palix, E. 2008. A global model for accurately interpreting CPT data in sands from shallow to greater depth. *In* Geotechnical and Geophysical Site Characterisation. *Edited by* A.B. Huang and P.W. Mayne. Taylor & Francis Group, London. pp. 687–694.

Engin, H.K., Khoa, H.D.V., Jostad, H.P., Kort, D.A., Bøgelund Pedersen, R., and Krogh, L. 2018. Large deformation finite element analyses for the assessment of CPT behaviour at shallow depths in NC and OC sands. *In* Proceedings of the 9th European Conference on Numerical Methods in Geotechnical Engineering (NUMGE 2018), Porto, Portugal. Vol. 1. CRC Press. pp. 611–619.

Jamiolkowski, M., Ghionna, V.N., and Lancellotta, R 1988. New correlations of penetration tests for design practice. *In* Proceedings of the International Symposium on Penetration Testing, ISOPT, Orlando. Balkema, Rotterdam. Vol. 1. pp. 263–296.

Jamiolkowski, M., Lo Presti, D.C.F., and Manassero, M. 2003. Evaluation of relative density and shear strength of sands from cone penetration test (CPT) and flat dilatometer (DMT). *In* Soil behaviour and soft ground construction. ASCE Geotechnical Special Publication 119. ASCE. pp. 201–238. doi:10.1061/40659(2003)7.

Kulhawy, F.H., and Mayne, P.W. 1990. Manual on estimating soil properties for foundation design. Report EPRI EL-6800, Electric Power Research Institute, Palo Alto.

Lee, J., Park, D., and Kyung, D., and Lee, D. 2013. Effect of particle characteristics on K_0 behaviour for granular materials. *In* Proceedings of the 18th International Conference on Soil Mechanics and Geotechnical Engineering, Presses des Ponts, Paris. pp. 337–350.

Lunne, T., Robertson, P.K., and Powell, J.J.M. 1997. Cone penetration testing in geotechnical practice. E&FN Spon Routledge.

Lunne, T., Knudsen, S., Blaker, Ø., Vestgården, T., Powell, J.J.M., Wallace, C.F., et al. 2019. Methods used to determine maximum and minimum dry unit weights of sand: Is there a need for a new standard? Canadian Geotechnical Journal, **56**(4): 536–553. doi:10.1139/cgj-2017-0738.

Masin, D. 2011. Ph.D. course on hypoplasticity. Faculty of Science, Charles University, Prague.

Mayne, P.W. 2009. Geoengineering design using the cone penetration test. ConeTec Inc., Richmond, B.C., Canada.

Puech, A., and Foray, P. 2002. Refined model for interpreting shallow penetration CPTs in sands. *In* Proceedings of the Offshore Technology Conference, Houston, Texas. Paper No. 14275.

Quinteros, V.S., Lunne, T., Dyvik, R., Krogh, L., Pedersen, R.B., and Rasmussen, S.B. 2017. Influence of pre-shearing on the triaxial drained strength and stiffness of a marine North Sea sand, Offshore Site Investigations and Geotechnics. *In* Proceedings of the 8th International Conference. Society for Underwater Technology, Vol. 1, London. pp. 338–345.

Quinteros, V.S., Lunne, T., Krogh, L., Pedersen, R.B., and Clausen, J.B. 2018. Shallow depth characterisation and stress history assessment of an overconsolidated sand in Cuxhaven, Germany. *In* Proceedings of the 4th International Symposium on Cone Penetration Testing (CPT'18), Taylor & Francis Group, Delft. pp. 525–531.

Santamarina, J.C., and Cho, G.C. 2001. Determination of critical state parameters in sandy soils – simple procedure. Geotechnical Testing Journal, **24**(2): 185–192. .doi:10.1520/GTJ11338J.

Senders, M. 2010. Cone resistance profiles for laboratory tests in sand. *In* Proceedings of the 2nd International Conference on Cone Penetration Testing, Huntington Beach, Calif. Paper No. 2-08.

Can. Geotech. J. Downloaded from cdnsciencepub.com by NORWEGIAN GEOTECHNICAL INSTITUTE (NGI) on 05/02/23

List of symbols

ALE arbitrary Lagrangian–Eulerian
a cone area ratio
B_q pore pressure parameter, $B_q = (u_2 - u_0)/(q_t - \sigma_{v0})$
C_0, C_1, C_2 fitting parameters for Ticino, Toyura, and Hokksund sands, respectively
C_C coefficient of curvature
C_U coefficient of uniformity
CADC anisotropic consolidated drained triaxial compression
CC calibration chamber
CEL coupled Eulerian–Langrangian
CPT cone penetration test
CPTU cone penetration test with pore pressure measurements
CRS constant rate of strain
D_{10} particle-size diameter for which 10% of sample is finer
D_{60} particle-size diameter for which 60% of sample is finer
D_c critical depth
D_r relative density, $D_r = (e_{max} - e)/(e_{max} - e_{min}) \times 100\%$
$D_{r,dry}$ relative density, dry conditions
$D_{r,sat}$ relative density, saturated conditions
DMT flat dilatometer test
e void ratio
e_{max} maximum void ratio
e_{min} minimum void ratio
FE finite element
f_s unit sleeve friction resistance
f_t sleeve friction corrected for pore pressure effects
GWT ground water table
K coefficient of earth pressure
K_0 coefficient of earth pressure at rest
K_P coefficient of passive earth pressure
L lateral extension of the slip lines and dimension of the cylinder
MASW multichannel analysis of surface waves
MD manual density
m' fitting exponent
NC normally consolidated
ND nuclear densometer (Troxler)
NGI Norwegian Geotechnical Institute
OC overconsolidated
OCR overconsolidation ratio
PLT plate loading test
p_a atmospheric pressure (= 100 kPa)
q_c cone resistance
q_{st} cone resistance at quasi-stationary state
q_t corrected cone resistance, $q_t = q_c + u_2(1 - a)$
q_{t1} stress normalized cone resistance, $q_{t1} = (q_t/p_a\sigma'_v)^{0.5}$
R particle roundness
R_f friction ratio, $R_f = (f_t/q_t) \times 100\%$ or $(f_s/q_t) \times 100\%$
S particle sphericity
SDMT seismic dilatometer test
SEM scanning-electro-micrograph
u_0 in situ pore-water pressure
u_2 pore-water pressure (measured at cone shoulder)
w water content
XRD X-ray diffraction
z depth
γ bulk unit weight
γ_d dry unit weight
$\gamma_{d,max}$ maximum dry unit weight
$\gamma_{d,min}$ minimum dry unit weight
γ_s unit weight of solid particles
ρ particle regularity
σ_v vertical total stress
σ'_h horizontal effective stress
σ'_m mean effective stress, $\sigma'_m = (\sigma'_v + 2\sigma'_h)/3 = (\sigma'_v/3)(1 + 2K_0)$
σ'_p past effective consolidation pressure or pre-consolidation pressure
σ'_v vertical effective stress
φ'_{cv} effective friction angle at constant volume
φ'_p effective peak friction angle
φ'_{rep} effective friction angle of repose